19th International Congress on Modelling and Simulation, Perth, Australia, 12–16 December 2011
http://mssanz.org.au/modsim2011

Analysis of Spectral Measurements in Paddy Rice Field: Implications for Land Use Classification

D. Ryu [a], **P. Teluguntla** [a], **H. Malano**[a], **B. George**[a], **B. Nawarathna**[a] **and A. Radha**[b]

[a]*Department of Infrastructure Engineering, The University of Melbourne, Parkville, Victoria, 3010*
[b]*International Water Management Institute, ICRISAT, Patancheru, Andhra Pradesh, India*
Email: dryu@unimelb.edu.au

Abstract: Rice is one of the most produced crops in the world consumed by over half of the entire population according to the FAOSTAT (2008). In addition to the agricultural value of rice, paddy-farming method used to grow rice raises a number of environmental issues, such as methane emissions and high fresh water consumption, associated with the production of rice. Monitoring of paddy fields at large scale is thus important to investigate their impacts on available water resources and greenhouse gas emissions as well as to predict and plan rice production of the year.

Due to the unique spectral features of paddy rice fields during the transplanting season (i.e., strong signals in the short-wave infrared range caused by the flooded soil of the paddy fields) the Land Surface Water Index (LSWI) has been used in conjunction with the Normalized Difference Vegetation Index (NDVI) to map paddy rice fields using satellite imagery (e.g., Xiao et al. (2005); Xiao et al. (2006)). To date, satellite images of spatial scales ranging from 30 m (e.g., Landsat) to 500 m (e.g., Moderate Resolution Imaging Spectroradiometer, MODIS) or coarser scales were directly compared with ground survey data to classify the land use in the mixed paddy rice and other cropping fields. However, due to the small size of typical rice fields in Asia where majority of rice fields are located, only a fraction of each satellite pixel is covered by the rice field. Moreover, the strong short-wave infrared signal from flooded soil may drop significantly as growing rice canopy masks signals from the background soil. In order to develop more sophisticated spectral models for satellite-based land use classification, these complex features of the paddy fields need to be analysed using measurements made directly on the rice fields in various growing stages.

We present spectral measurements collected during the Australia-India Land Surface Parameterisation Experiment for Remote Sensing (AILSPEX-RS1) conducted in February 2011 in the Musi catchment, India. Spectral signals at six wavelengths (i.e., 530, 570, 650, 855, 1240 and 1640 nm) were measured over 16 different land cover types during the local transplanting season of rice. Conditions of rice paddy fields varied from no-rice flooded soil to moderately grown rice canopies as tall as approximately 50 cm. LSWI of paddy rice linearly decreased with NDVI while the index in the non-paddy-rice fields increased linearly with NDVI. The linearly decreasing trend of LSWI of paddy rice continued until the NDVI values reached $\sim$0.8, after which LSWI of paddy rice increased with NDVI following the trend of the other crops. The analysis of the explicit NDVI-LSWI trends can be applied to map paddy rice fields until rice grows to $\sim$ 35 cm while the simple comparison of the indices by their magnitude can be applied to the paddy rice of approximately 20 cm.

Keywords: Remote sensing, land use classification, vegetation index, crop fields mapping, paddy rice

1 INTRODUCTION

Rice is consumed by over half of the entire population of the world (FAOSTAT, 2008). Due to the unique flooded-paddy farming methods of rice, accurate estimation of the paddy rice field is important to efficiently manage the food and water security as well as to plan on environmentally sustainable agriculture. Moreover, rice paddies are known to contribute over 15% of global methane emission; methane is one of the most significant greenhouse gases that poses a greater global warming potential (GWP) than carbon dioxide (i.e., 72 times greater in the period of 20 years and 25 time greater in 100 years) (Wahlen, 1993). Currently available land-cover and land-use maps based on satellite sensors, such as the global land cover maps based on the Landsat ETM+ and the Moderate Resolution Imaging Spectroradiometer (MODIS) produced by the Global Land Cover Facility (GLCF, `http://www.landcover.org/`), do not provide detailed sub-classification within the class of agricultural field.

However, the unique flooded farming method of rice can be utilised to discriminate the paddy rice fields from other agricultural fields. Particularly, during the transplanting season of rice, significant fraction of the rice paddies directly exposes the ponded water surface, resulting in strong water signal emitted from the surface. Even though the spectral signal from the ponded background is not readily observable using the optical bands in red and near infrared (NIR) regions, which are the most commonly used bands to classify the land cover types as well as to produce NDVI, the water signal can be captured by the Land Surface Water Index (LSWI, also called the Normalised Difference Water Index, NDWI). LSWI is calculated using the spectral signals in shortwave infrared (SWIR) and in NIR ranges to detect water at the soil surface (Chandrasekar et al., 2010) and the vegetation water content (Jackson et al., 2004). Previous works compared NDVI or the Enhanced Vegetation Index (EVI) with LSWI during the transplant season to map paddy rice fields in China, South and Southeast Asia (e.g., Xiao et al. (2002, 2005, 2006); Sun et al. (2009)).

Xiao et al. (2002) analysed the multi-temporal SPOT-4 satellite imagery (10-day composites of VEGETATION, 1-km resolution) collected over Jiangsu, China to map flooded paddy rice fields; pixels with NDWI greater than NDVI were classified as the paddy rice. Xiao et al. (2005) and Xiao et al. (2006) used the multi-temporal MODIS images (8-day composites, MOD09A1, 500-m resolution) to extend the approach to larger regions, south China, South and Southeast Asia. They used a relaxed set of criteria, LSWI+0.05 $\geq$ EVI or LSWI+0.05 $\geq$ NDVI, to identify flooded paddy rice fields. The mapped paddy rice fields were overall in good agreement with census statistics and regional land cover maps derived from the Landsat ETM+, although some discrepancies in land classes existed. The errors were attributed to the cloud contamination of optical images, topographic effects and low spatial-temporal resolution of the images. Sun et al. (2009) provided more detailed multi-year LSWI versus EVI relationships in paddy rice fields depending on the planting season of the crop.

Previous studies report that the coarse spatial and temporal resolution of satellite observations used is an important source of error in identifying flooded rice fields. The ground cover of rice increases steeply within a few weeks from transplanting and NDVI quickly saturates to its near-maximum values (Vaesen et al., 2001), leaving only a few windows of MODIS 8-day composites suitable for identifying rice fields. Moreover, due to the small size of paddy rice fields in South and Southeast Asian countries, most 500-m pixels feature mixture of flooded rice with non-flooded crops and vegetations, which degrades the performance of the paddy-rice-mapping algorithms based on the comparison of LSWI and NDVI (or EVI). Lack of detailed spectral samples collected under better controlled field conditions and intensive calibration/validation field campaigns for ground truth limit improvement of the algorithms. Note that the previous works reviewed developed algorithms directly on the satellite observations and the algorithms were calibrated and validated against the census statistics and higher-resolution satellite land cover products.

Motivated by the need of the ground-based spectral and biophysical samples to improve the paddy-rice-mapping algorithms, an intensive ground sampling was conducted as a part of the Australia-India Land Surface Parameterisation Experiment for Remote Sensing in 11-17 February 2011 (AILSPEX-RS1) in India. During the experiment, spectral reflectance at six wavelengths, 530, 570, 650, 855, 1240 and 1640 nm, was measured with ancillary data (e.g., surface soil moisture, crop height, soil and vegetation canopy temperatures, etc.) at 42 sites of 16 land cover types. The experiment period captured the transplanting

season of *Rabi* (winter, dry cropping season) rice in the region. LSWI and NDVI are produced over the paddy rice fields and surrounding non-flooded crop fields, and analysed with varying crop height. Our hypothesis is that the explicit NDVI versus LSWI relationship of paddy rice fields displays distinct features from the other crop fields during the transplanting season, gradually decreasing LSWI with the growth of rice. We also hypothesise that mapping rice paddies can be more effectively done by analysing the evolution of LSWI-NDVI relationship with the crop growth than simply comparing the indices.

2 STUDY SITE

AILSPEX-RS1 was conducted at two sampling areas located in the Musi catchment, Inida (see Sampling Sites 1 and 2 in Figure 1). The Musi River is a principal tributary of the Krishna River located in Southern India, and the Musi catchment lies between longitudes 77°50′E to 79°43′E and latitudes 16°43′N to 17°53′N. The total geographical area of the catchment is approximately 11,000 km^2 (Central Water Commission of India, `http://www.cwc.nic.in/`). The river originates in the Ananthagiri hills around 100 km west of Hyderabad in Andhra Pradesh and flows around 250 km towards east then merges into Krishna River at Damarcherala. The climate of the Musi catchment is dominantly of semi-arid. The mean annual rainfall of the catchment is 750 mm and 90% of precipitation occurs during the monsoon months of June–October and is unevenly distributed in both spatially and temporally. The land use of the catchment is highly heterogeneous and has a relatively diversified cropping pattern. Average size of the agricultural land is approximately 0.5 ha and cropping pattern occurs in two seasons named *Kharif* (monsoon, summer) and *Rabi* (dry, winter). The major land uses are agriculture (rainfed, irrigation with surface water and ground water), forest, urban, barren and rocky areas. Most of fields under rainfed agriculture are cultivated by single crops (i.e., single harvest for each year) and the areas with irrigation facility are getting two crops per annum. The major crops include rice followed by vegetables, sorghum, millets, cotton, chilies, maize, grams, ground nuts, sugar cane, and fodder grass.

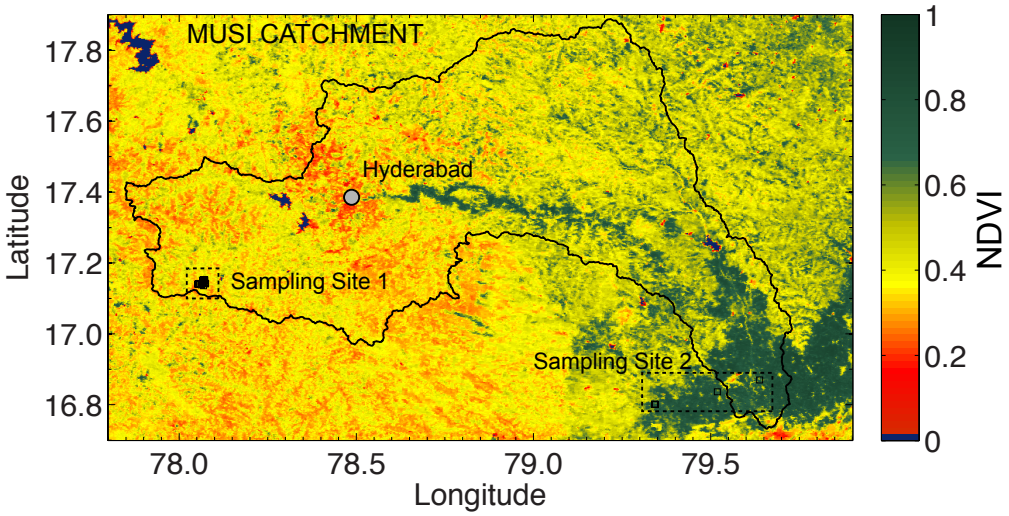

Figure 1. Location of the sampling sites in the Musi catchment. Sampling locations are marked in squares.

Figure 1 shows the catchment boundary and the two AILSPEX-RS1 sampling sites superimposed on the 16-day NDVI composite image collected during the campaign (49th Julian date in 2011) from Terra (MOD13Q1). The first sampling site is located near Tekulapalle (watershed area), and Uttarajepalle villages of Kondurg mandal in Mahabubnagar District, Andhra Pradesh, which is in the south west part of the upper Musi catchment (Sampling Site 1 in Figure 1). Majority of agriculture practice in the Sampling Site 1 is under rainfed with supplemented groundwater irrigation. The Sampling Site 2 is composed of a selection of sparse sampling spots in the downstream of the Musi catchment, the south east part of the catchment, where the agricultural practice is mostly under surface irrigation. Three sampling

locations exist outside of the Musi catchments for logistic purposes, however, they represent the surface-water-irrigated rice paddies of the area. The experiment period (11-17 February in 2011) captured the transplanting season of Rabi rice in the upper Musi catchment, near the Sampling Site 1. However, the transplanting season of the surface-water-irrigated paddy fields (i.e., downstream Musi catchment around the Sampling Site 2) precedes that of the rainfed/groundwater-irrigated fields in the upper Musi catchment by a few weeks. The gap in the timing of transplant resulted in the rice in the Sampling Site 2 grown up to 35-50 cm during the AILSPEX-RS1 period while the height of rice in the Sampling Site 1 ranged from 0 (prior to transplanting) to 20 cm. The variation of the growth stages of rice provided a good opportunity to collect the spectral samples of paddy rice under diverse biophysical conditions during the relatively short period of the campaign. Among a total of 42 sampling locations, four locations (3 paddy rice fields and 1 open water) are in the Sampling Site 2 and the others (38 locations) are in the Sampling Site 1. Sixteen land use types of the sites are summarised in Table 1. Note that the listed land uses comprise only 36 sampling sites that are used for the analyses in this work; samples taken at 6 sites (deep-water bodies and bare soils) are not used, thus they are not listed in the table.

Table 1. Summary of land uses the number of sites in the sampling locations

Land Use	No. of Sites	Land Use	No. of Sites
Rice	10	Open Water	2
Fallow/Bare Soil	4	Maize	3
Chilli	2	Eggplant+Spring Onion	2
Sorghum	1	Cotton (Harvested)	3
Turmeric	1	Sugarcane	1
Jowar	1	Carrot	1
Wheat	1	Dry Grass	2
Pigeonpea	1	Weeds	1

3 DATASETS AND METHODS

During AILSPEX-RS1, field measurements were taken at 42 sampling locations of 16 different land uses. The ground data collected include 12-band reflectance measurements by CROPSCAN (model MSR16 by CROSCAN, Inc.), surface skin temperature, soil temperature values at the top 1 cm, 5 cm and 10 cm, vegetation height, soil moisture content at the top 5 cm by the theta probe soil moisture sensor (model ML2 by Delta-T Devices Ltd.). Two temporary weather stations were installed in the Sampling Site 1, which collected the standard meteorological measurements at 30-minute intervals. Spectral bands of the CROPSCAN are listed in Table 2; two sets of the listed 6 bands (12 bands in total) are set to face the sky and the ground, respectively, for the on-site calibration. Two normalised indices, NDVI and LSWI, are calculated for analyses using three bands, B3 (650 nm), B4 (855 nm) and B6 (1640 nm), as follows:

$$\text{NDVI} = \frac{B4 - B3}{B4 + B3}, \qquad \text{LSWI} = \frac{B4 - B6}{B4 + B6}.$$

Since our study focused on the paddy rice fields, about 25% of the entire measurements were collected from the rice fields (10 locations out of 42 in total). At each sampling location, 5 ground measurements were taken considering the small scale spatial variation. Whereas the Sampling Site 2 was composed mostly of the surface-water-irrigated rice fields, the Sampling Site 1 had small patches of fields with various crop types. The non-rice crops ranged from dry grass and young spring onion to tall maize and sugarcanes (see Table 1). For the comparison of the normalised indices, the crop types are grouped simply into two categories: rice and non-rice crops/vegetations (excluding tree vegetations). It is assumed that the non-rice crops/vegetations in the non-flooded seasons share common spectral features for the normalised indices distinct from the paddy rice. Based on the assumption, two linear models are fit to the NDVI versus LSWI of the dataset in two categories separately (Figure 2). By visually analysing the plots, it is assumed that the paddy rice have a unique spectral feature until NDVI reaches approximately 0.8 (see blue circles in Figure 2a), thus only the measurements at the rice fields with NDVI lower than 0.8 are

used for the model fitting. In order to investigate the correlation between the indices and the height of rice, NDVI and LSWI are fit against the height of rice separately and two linear models are fit to the data separately (Figure 2).

Table 2. Spectral bands of the CROPSCAN (MSR16R) and equivalent bands of MODIS

Bands	Centre Wavelength (nm)	Band Width (nm)	Sub-division	MODIS Bands
B1	530	8.5	VIS*	Band 11
B2	570	9.7	VIS	None
B3	650	40.0	VIS	Band 1
B4	855	40.0	NIR†	Band 2
B5	1240	11.6	NIR	Band 5
B6	1640	15.5	SWIR‡	Band 6

*Visible Bands, †Near Infrared Bands, ‡Shortwave Infrared Bands

4 RESULTS AND DISCUSSION

Analyses of this work mainly focus on the comparison of the distinct features of NDVI-LSWI between the paddy rice and the other non-flooded crop/vegetation fields. Figure 2a summarises the spectral responses from the two categorised fields. LSWI of the non-rice crops increases with NDVI in general on a linear trend. The strong linear relationship (correlation coefficient = 0.94) between the indices is due to the dominant impact of the vegetation water content on the observed LSWI in the non-rice fields, which is also strongly correlated with NDVI. Surface soil moisture content varied between 0.0288 m^3m^{-3} and 0.4220 m^3m^{-3} in the non-rice fields, however, neither NDVI nor LSWI exhibited noticeable correlation with soil moisture (results are not shown here).

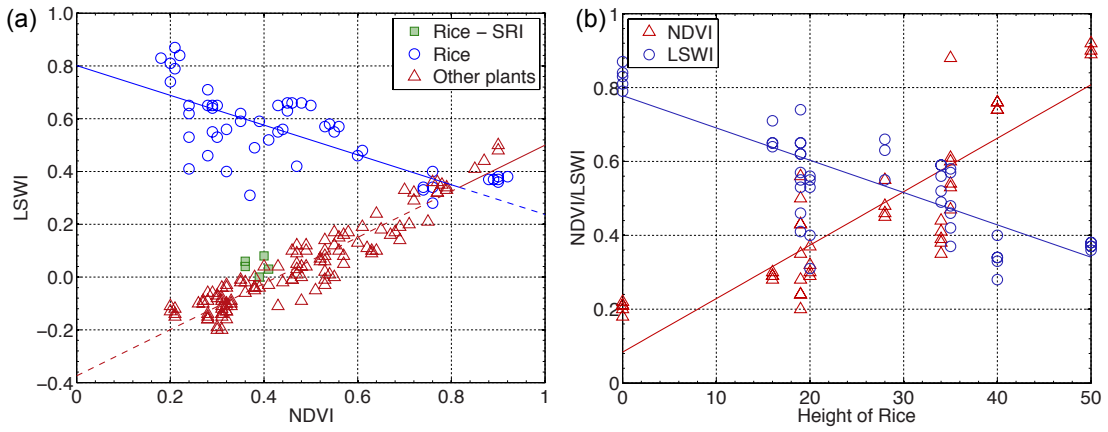

Figure 2. (a) Comparison of NDVI and LSWI collected in the paddy rice and the other non-flooded crop/vegetation fields. (b) Comparison of NDVI and LSWI with the height of rice. All the spectral samples are collected in the paddy rice fields.

In contrast with the other non-flooded crops and vegetations, LSWI of the paddy rice fields shows decreasing trend with NDVI. Even though LSWI is scattered widely around the linear fit (see Table 3 for the summary statistics of errors), LSWI decreases linearly with NDVI until the NDVI of rice reaches approximately 0.8. The two linear models intersect where NDVI is 0.8173. It also appears that LSWI of paddy rice joins the increasing trend with NDVI beyond the threshold NDVI value. The decreasing trend is mainly due to that fact that the spectral signal coming directly from the ponded surface in the background decreases with the growth of rice. It is worth noting here that the Sampling Site 1 included a rice

field that was managed by the System of Rice Intensification (SRI). Typically in the SRI rice fields, crops are given "just enough water" to meet the minimum requirements (Uphoff et al., 2011). In the sampled SRI field, soil surface was not ponded although it was in near-saturation condition. The green squares in Figure 2a show that the LSWI of the SRI rice field behaves rather like the values from the non-rice fields. For paddy rice fields, the decreasing LSWI with NDVI is highly correlated with the height of rice (Figure 2b).

Analysis of the results in Figure 2 also shows that examining the trends between NDVI and LSWI is more informative for discriminating paddy rice fields that simply comparing the magnitude of the normalised indices that was adopted by the previous works (e.g., Xiao et al. (2005, 2006); Sun et al. (2009)). Although the Figure 2b is produced solely using the indices from the paddy rice fields, the LSWI values are greater than NDVI only up until the height of rice reaches approximately 20 cm. On the other hand, the spectral samples from the paddy rice exhibit clear distinction from the values of the other fields up to NDVI = 0.6, which is equivalent to 35 cm of rice crop height. The observed difference in the crop height range feasible for discriminating paddy rice fields can have an important implications when it is interpreted into the feasible period of the year to map the rice fields. With given limits in temporal scales of satellite images (when using the 8-day composite imagery of MODIS) for mapping, the larger time windows for mapping gained by the explicit LSWI-NDVI analysis may significantly improve the mapping capability of rice fields. In addition to the advantages in the feasible time windows, comparison of the plots in Figure 2 implies superior performance of the explicit LSWI-NDVI analysis for mapping when it is assumed that the rice grows linearly with time just after transplanting. Plots of paddy rice in Figure 2a can be better separated from the other fields while a number of LSWI and NDVI values are mixed when the height of rice is greater than 10 cm.

Table 3. Summary of model parameters[†] and error statistics

Crop	x	y	a	b	R^2	RMSE
Paddy Rice	NDVI	LSWI	-0.5645	0.8016	0.44	0.1066
Non-rice Crops	NDVI	LSWI	0.8741	-0.3742	0.89	0.0544
Paddy Rice	Crop Height	NDVI	0.0145	0.0839	0.76	0.1094
Paddy Rice	Crop Height	LSWI	-0.0087	0.7782	0.62	0.0913

[†]Linear model: $y = ax + b$

5 CONCLUSIONS

Comparison of LSWI with NDVI has been used as an important tool to map paddy rice fields. While the previous studies used a simple comparison of magnitudes in the normalised indices, it is hypothesised that the mapping can be conducted more effectively by examining the explicit evolution of NDVI-LSWI relationship with the growth of rice. Base on the comparison of the normalised indices between the paddy rice and non-paddy-rice fields, the following conclusions are derived: i) LSWI of paddy rice linearly decreases with NDVI while the index linearly increases with NDVI for non-paddy-rice fields; ii) The linearly decreasing trend of LSWI continues until the NDVI of rice reaches ∼0.8 (which is equivalent to the crop height of approximately 40 cm); iii) SRI rice behaves like the other non-paddy-rice crop in NDVI vs. LSWI trend; iv) explicit analysis of the indices outlined in this work is superior to the simple comparison of their magnitudes in terms of the feasible period of the year and the capability of discriminating rice paddies.

Practical utility of approach introduced in this work needs to be tested using the actual satellite imagery. Heterogeneity of the land cover types within a typical scale of the satellite pixels (∼500 m for MODIS) may significantly degrade the utility of our approach. Application of the analysis to map paddy rice fields in the Musi catchment is currently in progress along with a planning of AILSPEX-RS2 to capture more diverse land surface conditions and seasons.

ACKNOWLEDGEMENT

This research was generously supported by the ACIAR Project LWR-2007-113, *'Impacts of climate change and watershed development on whole-of-basin agricultural water security in the Krishna Basin, India and Murray-Darling Basin, Australia'*. The authors would also like to thank the supports by the ECO club and the assistance in the field by our driver, 'Ajay'. The hospitality of the International Water Management Institute (IWMI) during the experiment is gracefully acknowledged.

REFERENCES

Chandrasekar, K., M. V. R. Sesha Sai, P. S. Roy, and R. S. Dwevedi (2010). Land Surface Water Index (LSWI) response to rainfall and NDVI using the MODSI Vegetation Index product. *International Journal of Remote Sensing 31*(15), 3987–4005.

FAOSTAT (2008). FAOSTAT 2008. http://faostat.fao.org/.

Jackson, T. J., D. Chen, M. Cosh, F. Li, M. Anderson, C. Walthall, P. Doraiswamy, and R. Hunt (2004). Vegetation water content mapping using Landsat data derived normalized difference water index for corn and soybeans. *Remote Sensing of Environment 92*, 475–482.

Sun, H., J. Huang, A. R. Huete, D. Peng, and F. Zhang (2009). Mapping paddy rice with multi-date moderate-resolution imaging spectroradiometer (MODIS) data in China. *Journal of Zhejiang Unviersity Science A 10*(10), 1509–1522.

Uphoff, N., A. Kassam, and R. Harwood (2011). SRI as a methodology for raising crop and water productivity: productive adaptations in rice agronomy and irrigation water management. *Paddy Water Environment 9*, 3–11.

Vaesen, K., S. Gilliams, K. Nackaerts, and P. Coppin (2001). Ground-measured spectral signatures as indicators of gorund cover and leaf area index: the case of paddy rice. *Field Crops Research 69*, 13–25.

Wahlen, M. (1993). The global methane cycle. *Annual Review of Earth and Planetary Sciences 21*, 407–426.

Xiao, X., S. Boles, S. Frolking, C. Li, J. Y. Babu, W. Salas, and B. Moore III (2006). Mapping paddy rice agriculture in South and Southeast Asia using multi-temporal MODIS images. *Remote Sensing of Environment 100*, 95–113.

Xiao, X., S. Boles, S. Frolking, W. Salas, B. Moore III, C. Li, L. He, and R. Zhao (2002). Observation of flooding and rice tranplanting of paddy rice fields at the site to landscape scales in China using VEGETATION sensor data. *International Journal of Remote Sensing 23*(15), 3009–3022.

Xiao, X., S. Boles, J. Liu, D. Zhuang, S. Frolking, C. Li, W. Salas, and B. Moore III (2005). Mapping paddy rice agriculture in southern China using multi-temporal MODIS images. *Remote Sensing of Environment 95*, 480–492.